Hindawi
International Journal of Aerospace Engineering
Volume 2021, Article ID 5521455, 8 pages
https://doi.org/10.1155/2021/5521455

Research Article

The Influence Factors of Grain Integrity under the Internal Pressure Condition in SRM

Chunguang Wang[1] **and Weiping Tian**[2]

[1]*State Key Laboratory for Strength and Vibration of Mechanical Structures, School of Aerospace Engineering, Xi'an Jiaotong University, Xi'an 710049, China*
[2]*The Fourth Academy of China Aerospace Science and Technology Corporation, Xi'an 710025, China*

Correspondence should be addressed to Weiping Tian; tianweiping1964@163.com

Received 28 January 2021; Revised 3 June 2021; Accepted 18 July 2021; Published 16 August 2021

Academic Editor: Marco Pizzarelli

To investigate the influence factors of propellant grain integrity under the internal pressure, the cylindrical grain was equivalent to a thick-wall cylinder and its three-dimension stress-strain problem was solved. Under the internal and external pressure, the strain and displacement equations of the inside thick-wall cylinder were expressed, and then, the stress and strain expressions of grain were obtained. On this basis, the hoop strain equations on the inside surface of the cylindrical grain and case were developed. The hoop strain on the inner surface of the grain can be predicted by the hoop strain of the case cylinder via the strain equations, and therefore, the hoop strain in the inner surface can be indirectly monitored in real time during the working process of the motor. The hoop strain in the inner surface of grain can be effectively reduced by increasing the case stiffness or decreasing the m number of the grain.

1. Introduction

The load conditions that the grain in solid rocket motor (SRM) experiences during the stages from production to flight are temperature load in the stage of propellant solidify, gravity load in storage stage, inner pressure when a motor is in working process, and the inertia load in the flight stage [1, 2]. Given that the grain structure is rationally designed, when the comprehensive mechanical properties of propellants are good or the working temperature is not very low, the structural integrity of grain usually can be ensured under the working pressure [3]. Also, the influence from the case stiffness is not obvious, and the case design can meet the requirement of the internal pressure strength will be enough [4–6]. As for tactic motors in service at low temperatures, explosions occur from time to time in the ground test when the motor is working [7, 8]. In this regard, on the one hand, people believe that this is related to the decrease of the overall mechanical properties of the propellant at low temperatures. For instance, the fracture strain and fracture toughness of the grain reduce at low temperatures, while its fracture strength increases indicating that the tendency of its brittleness property is noticeable. On the other hand, when mechanical properties of the propellant at low temperatures are enhanced, the influence of the grain *m* number, internal pressure, boost rate, and case stiffness on the structural strength of the propellant grain should be considered in the motor design [9–12].

The hoop strain on the inner surface is a significant indicator of propellant grain form design for SRMs. It is not only related to the reliability of the grain structure but also the basis for determining the m number of grains. Limited to the measurement methods of the strain of grains, the strain on the inner surface of grains cannot be tested, and predictive results given by the elastic solution cannot be verified by the ground tests, so it is inevitable to design it too safely and conservatively [13].

The influence of case stiffness on the grain strength under inner pressure is discussed in this paper. To analyze the influence of the case on grains, the combination of the case and grains as an integral whole is necessary to study mechanical properties under inner pressure. The viscoelastic mechanical

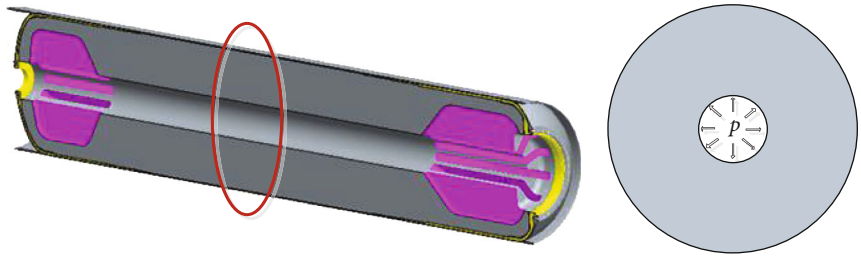

Figure 1: The scheme of the grain structure in solid rocket motors.

method should be applied to the accurate analysis of viscoelastic propellant grains, but it is difficult to obtain an analytical solution in such conditions. However, the elastic property of grains is remarkable under rapid pressure loading, and when it is considered as an elastic body, the result is accurate sufficiently [14].

The elastic mechanical method was employed in this paper to obtain the analytical solutions for quantitative and qualitative analysis, which was to analyze and discuss the mechanical properties of circular tube grains under internal pressure considering the case stiffness of materials [15–17]. The relation between the hoop strain on the inner surface of circular tube grains and the hoop strain of the case under inner pressure was deduced, and the accuracy of the expression was verified by the finite element method and ground tests [18, 19]. The research results show that it is viable to predict the hoop strain on the inner surface of the tube grain from the case strain [20–23]. The conclusion drawn in this paper can be applied to the analysis and design of SRMs.

2. The Strain of the Grain

The tube section in the middle part of the grain is intercepted as a research subject, as shown in Figure 1. Under the internal pressure load p, the pressure q between grains and cases is computed by Equation (1), and the specific derivation process is elaborated in literature 15 and literature 16.

$$q = \frac{4(1-\upsilon^2)P}{2(1+\upsilon)[1+(1-2\upsilon)m^2]+(2-\upsilon_k)(m^2-1)(ER/E_k h)}, \tag{1}$$

where $m = R/a$ is the ratio of the outer diameter to the inner diameter of the grain, p is the internal pressure, υ is Poisson's ratio of the grain, E is the elastic modulus of the grain, υ_k is Poisson's ratio of the case, and E_k is the elastic modulus of the case. If it is a composite material case, υ_k is circumferential-longitudinal Poisson's ratio, and E_k is the circumferential elastic modulus.

After obtaining q, the strain at any point of the grain can be acquired by following Equation (2), in which r is the polar coordinate of a point inside the grain.

$$\varepsilon_r = \frac{1+\upsilon}{(m^2-1)E}\left\{\left[(1-2\upsilon)-\frac{R^2}{r^2}\right]p+\left[\frac{R^2}{r^2}-(1-2\upsilon)m^2\right]q\right\},$$
$$\varepsilon_\theta = \frac{1+\upsilon}{(m^2-1)E}\left\{\left[(1-2\upsilon)+\frac{R^2}{r^2}\right]p-\left[\frac{R^2}{r^2}+(1-2\upsilon)m^2\right]q\right\}. \tag{2}$$

Besides, according to the research [17–19], Poisson's ratio of grains approximates 0.5. Substitute $\upsilon = 0.5$ and $r = a$ (coordinates on the inner surface of grains) into Equation (2), and the strain on the inner surface of grains will be as following:

$$\varepsilon_r = \frac{1.5m^2}{(m^2-1)E}(q-p),$$
$$\varepsilon_\theta = \frac{1.5m^2}{(m^2-1)E}(p-q). \tag{3}$$

The pressure between grains and the case in Equation (1) can be simplified as

$$q = \frac{3P}{3+(2-\upsilon_k)(m^2-1)(ER/E_k h)}. \tag{4}$$

According to the continuity condition of displacements, it can be known that the strain of the grain will be equal to the strain of the case at the bonding point between the grain and the case, that is, at $r = R$. Therefore, substitute $r = R$ and $\upsilon = 0.5$ into Equation (2), and the strain of the case will be expressed as follows:

$$\varepsilon_r^k = \frac{1.5}{(m^2-1)E}(q-p),$$
$$\varepsilon_\theta^k = \frac{1.5}{(m^2-1)E}(p-q). \tag{5}$$

By comparing Equations (5) and (3), the strain of the tube section on the case and the strain of the grain on the inner surface can be elaborated as Equation (6).

$$\varepsilon_r = m^2\varepsilon_r^k,$$
$$\varepsilon_\theta = m^2\varepsilon_\theta^k. \tag{6}$$

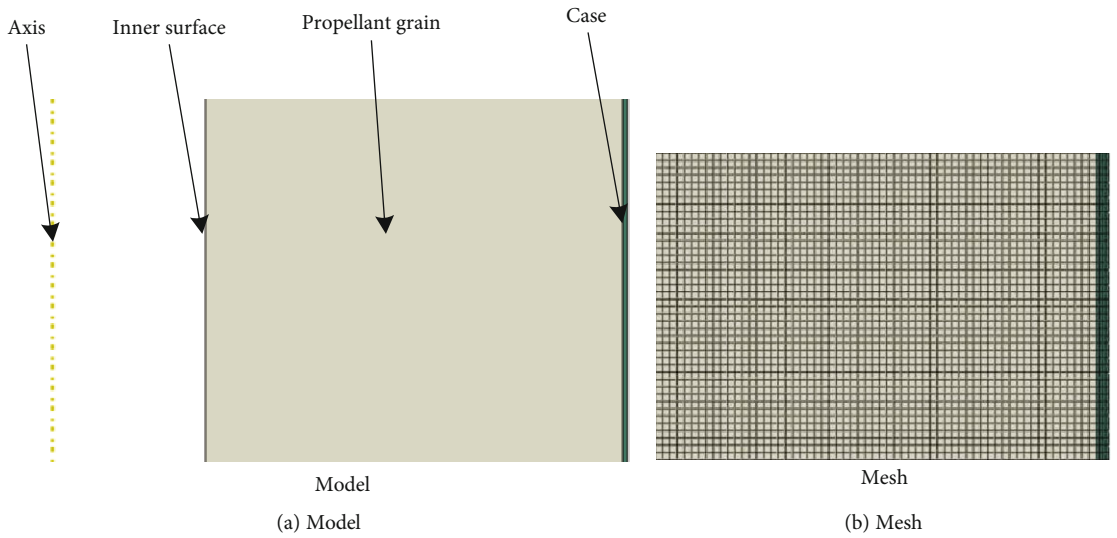

Figure 2: The model of numerical calculation.

Equation (6) is deduced under the quasi-static loading condition. During the working process of the motor, it can be regarded as a quasi-equilibrium state at any time, which indicates that Equation (6) is valid at any time.

The hoop strain of the tube section, either in the case or in the grain structure, is much greater than the axial strain, and because of the space limitation, the influence factor on hoop strain on the inner surface of grain is only discussed in this paper [16, 20].

The m number of the grain is a function of decreasing with motor working time, it reaches the largest when $t = 0$. Hence, if there is an initial pressure peak of the motor, at the corresponding moment, the hoop strain of the case is the largest, and the hoop strain of the grain is also the largest at this time, as shown in Equation (7). This is also the reason that the ignition timing of the motor at low temperatures is very dangerous.

$$\varepsilon_{\theta\ \max} = m^2 \varepsilon^k_{\theta\ \max} = m^2 \frac{Rp_{\max}}{2E_k h}(2 - \upsilon_k). \tag{7}$$

The hoop strain of the case is as following [20]:

$$\varepsilon^k_\theta = \frac{Rp}{2E_k h}(2 - \upsilon_k). \tag{8}$$

3. Numerical Validation

The tube section of a SRM was intercepted and its two-dimensional axisymmetric finite element model was established to validate the accuracy of Equations (3) and (4), as shown in Figure 2. The diameter of the case is 750 mm, and the wall thickness of case is 3.5 mm; while the inner diameter of the grain is 200 mm, and the internal pressure is 7.4 MPa. The material parameters are shown in Table 1. In this paper, the hybrid element CAX4RH in ABAQUS was used to avoid the self-locking problem of the high Poisson's ratio of grain.

Table 1: Property parameters of the case and the grain.

Structure components	Modulus	Poisson's ratio
Case	206 GPa	0.285
Grain	0.7 MPa	0.5

The calculation results of the internal strain of the grain are shown in Figure 3, and the variation trend of the strain along the radius is shown in Figures 3 and 4. It can be seen from the figures that results calculated from Equation (3) are consistent greatly with the numerical simulation results, while the numerical results are slightly larger than the calculated value of Equation (3). The reason is that the change of the m number resulting from the deformation of the inner hole in the grain is not considered in the calculation, which affected the calculation result to be smaller.

The strain curve in the figure shows that the strain inside the grain is changing from the inner surface of the grain column to the surface of the case. The reason is that under the action of internal pressure, the diameter of the inner surface of the grain expands and becomes larger, leading to the maximum hoop tensile strain on the inner surface, which gradually decreases along the radial direction and tends to a constant value when approaching the case. In the radial direction, the inner surface of the grain is compressed, and the radial strain is mainly compression strain, all of which are negative. The closer to the case, the closer the value is to the fixed value.

Based on Equation (4), the internal pressure between the grain and the case is $q = 7.38$ MPa, and the result calculated from the numerical model is also 7.38 MPa, as shown in Figure 5, which shows that Equation (4) has a high calculation accuracy.

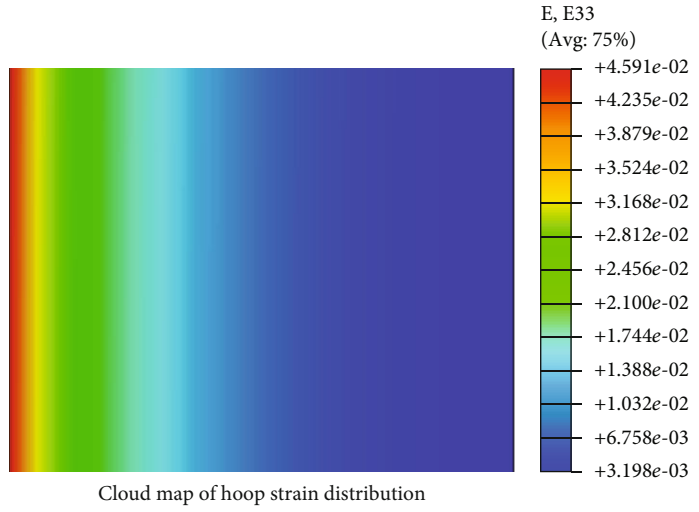

Cloud map of hoop strain distribution

(a) Cloud map of hoop strain distribution

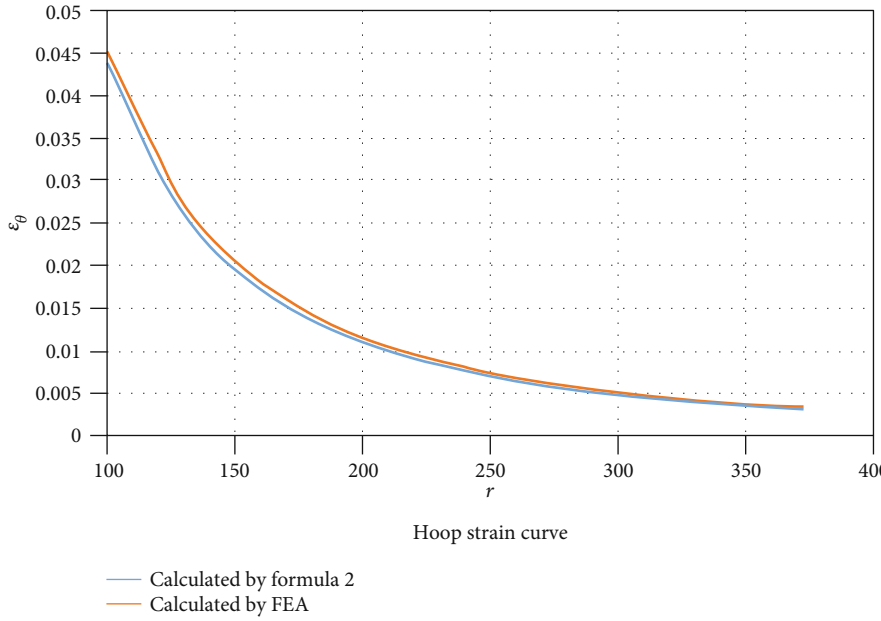

Hoop strain curve

(b) Hoop strain curve

Figure 3: The result of the hoop strain calculated.

4. Ground Test

The strain change in the outer surface of the motor case was monitored during one ground test, which was to verify the accuracy of strain calculation of the motor case so that it can provide support for indirect measurement of the strain of the grain.

In the motor ground test, the change tendency of the pressure in the combustion chamber and the hoop strain of the tube section of the case is shown in Figure 6. It can be figured out that the strain measured by the ground test is in good agreement with the calculation result by equations.

The working time of the motor is 46.8 s. During the whole working process, the m number decreases with the regression of the propellant grain surface. It is necessary to obtain the change rule of the grain thickness according to the relationship between pressure and time. Consequently, the variation rule of the m number over time of the motor working process was obtained, substitute which into Equation (6), and the change of the hoop strain of the grain was acquired as shown in Figure 7.

It can be seen that the variation tendency of the hoop strain of grain in the motor is consistent with the changing trend of the m number. At the commence of the motor working process, the hoop strain of the inner hole in the grain is the largest, which is the moment of highest risk, while along with the regression of the combustion surface of grain, the strain of the inner hole of the grain decreases rapidly. This result validates the conclusions in previous papers [19, 20].

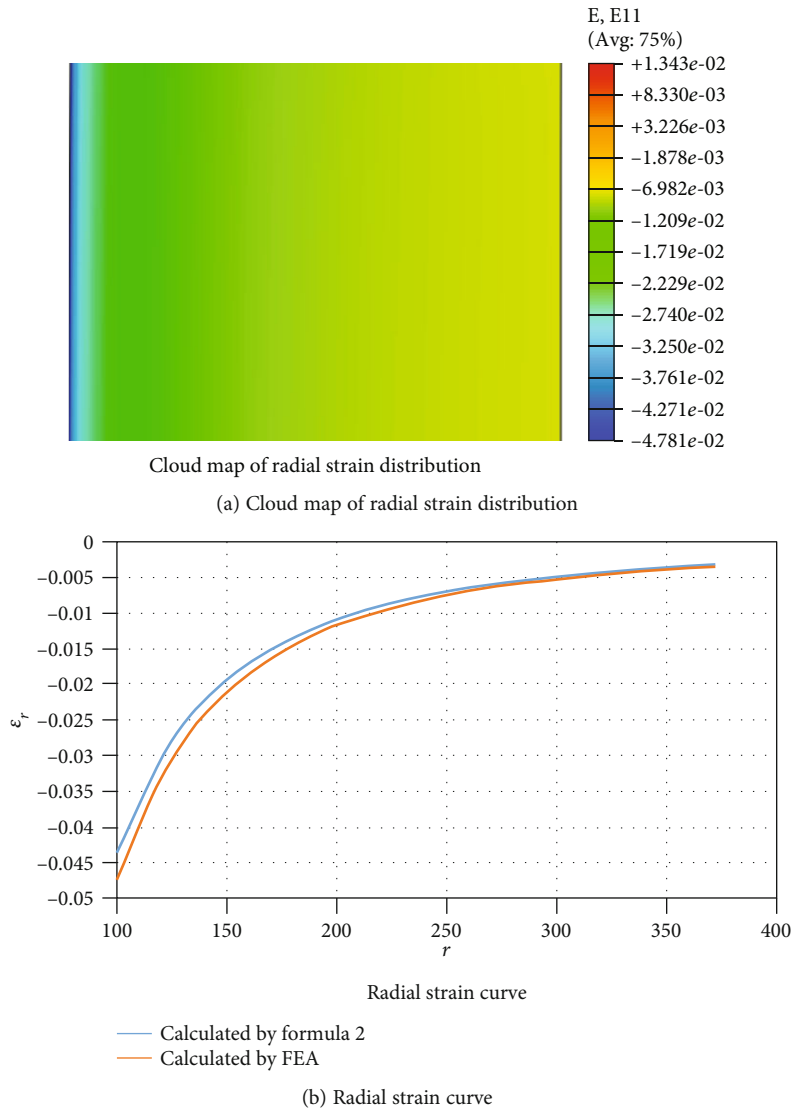

Figure 4: The result of the radial strain calculated.

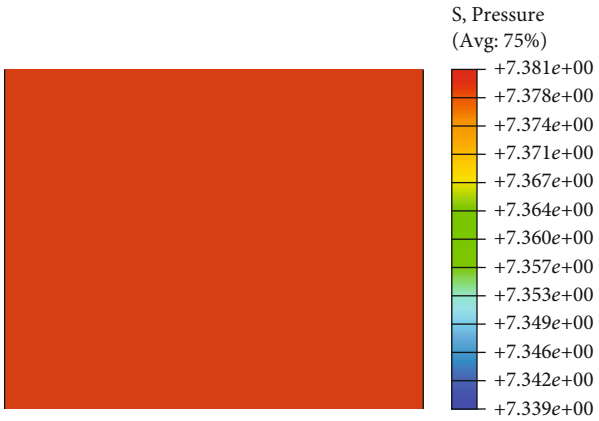

Figure 5: The pressure distribution of the grain.

5. Discussion

(1) The fracture strain of grains is low at low temperatures. If the maximum tensile strain criterion is used to verdict the strength failure of the grain, the hoop strain on the inner surface of the grain should be decreased to the greatest extent. It can be seen from the second equation in Equation (3) that ε_θ can be effectively reduced by the growth of pressure q between the grain and the case. To increase q, it is not difficult to obtain a solution as long as Equation (1) of q is analyzed carefully

(2) Both the decrease of m, E, and R and the increase of υ_k, E_k, and h can make q increase based on Equation (1). This indicates that to ensure the strength of the grain at low temperatures, the m number and the modulus E of the grain should not be too large when designing the grain. In the case design, the materials

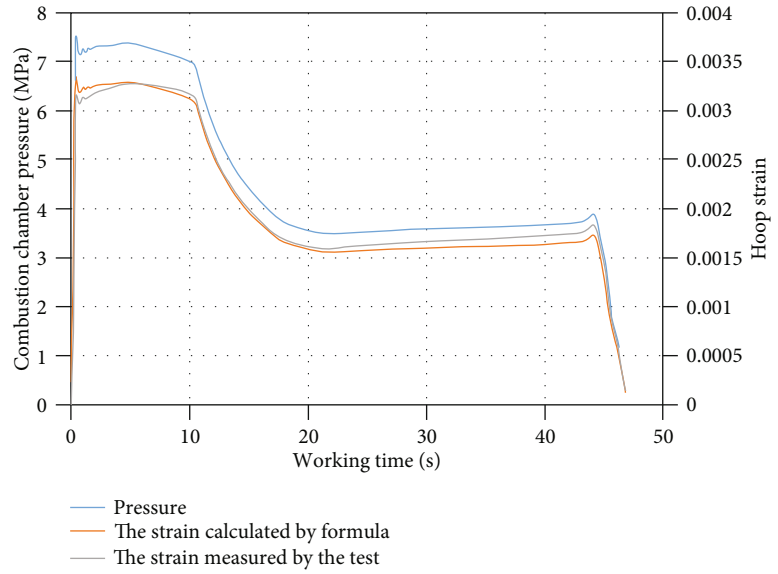

Figure 6: The change tendency of the hoop strain of the case during the motor working process.

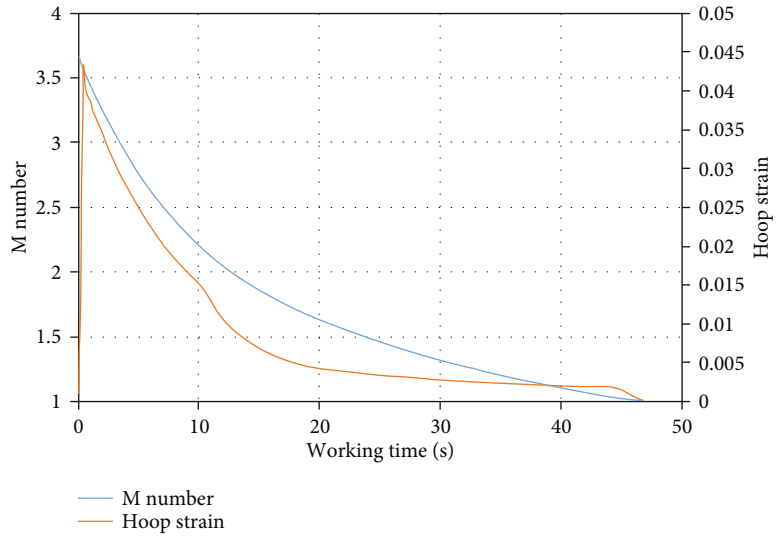

Figure 7: The change of m number and the hoop strain of inner hole over time.

with larger hoop modulus and Poisson's ratio should be selected as a priority

(3) It can be seen from Equation (7) that the hoop strain of the case is inversely proportional to $E_k h$. $E_k h$ usually is called case stiffness, the increment of which can effectively reduce the hoop strain on the inner surface of the grain. However, the growth of the cylindrical wall thickness will increase the case mass, which will reduce the mass ratio of the motor

(4) According to Equation (7), the initial pressure peak at commencing of the motor working process has a great impact on the integrity of the grain. Therefore, when design the grain, the existence of the initial pressure peak should be avoided, and the time when the maximum working pressure occurs should be delayed as far back as possible

(5) Based on the second equation in Equation (6), the m number can be expressed as

$$m = \sqrt{\frac{\varepsilon_\theta}{\varepsilon_\theta^k}}. \tag{9}$$

The hoop strain of grain is taken as the allowable strain $[\varepsilon] = \varepsilon_{g\ \max}/k$, where $\varepsilon_{g\ \max}$ the fracture strain of the propellant grain and k is a safety factor. Then, introducing Equation (8), the strain of the case and $\varepsilon_{\theta\ \max}^k = (Rp_{\max}/2E_k h)(2 - \upsilon_k)$ is

obtained. Thus, Equation (9) converts into the following form:

$$m = \sqrt{\frac{2E_k h[\varepsilon]}{Rp_{\max}(2-\upsilon_k)}}. \tag{10}$$

It can be known from Equation (10) that the determination of m number of grains is not only determined by the fracture strain of the propellant but also closely related to the case stiffness, the diameter of the case, and maximum working pressure of the motor.

According to the second equation in Equation (6), under the maximum working pressure condition, the hoop strain of the case must meet the following equation so that the hoop strain of the inner surface of the grain will not exceed its allowable strain $[\varepsilon]$

$$\varepsilon_\theta^k \le \frac{[\varepsilon]}{m^2}. \tag{11}$$

Substitute it into the strain of the case and we can obtain the following:

$$\frac{Rp_{\max}}{2E_k h}(2-\upsilon_k) \le \frac{[\varepsilon]}{m^2}, \tag{12}$$

$$E_k h \ge \frac{Rp_m m^2}{2[\varepsilon]}(2-\upsilon_k). \tag{13}$$

For the steel case, Equation (13) can generally be satisfied, because the elastic modulus of steel E_k is large. For composite cases, especially for the glass fiber-reinforced composite cases, due to their small elastic modulus, sometimes Equation (13) may not able to be satisfied, higher requirements for the elastic modulus E_k of which are put forward.

6. Conclusion

(1) During the motor working process, both inner pressure and m number are functions of time, so the strain of grains is not only a function of radial coordinate r but also a function of time. Under the internal pressure loading, the hoop strain on the inner surface of the grain is into tension strain, which is a significant parameter affecting the structural integrity of the grain. The method to determine the m number of the inner hole of the grain is elaborated in this paper. The m number is not only a function of grain performance but also a function of the maximum working pressure of the motor, geometric dimensions of the case, and material properties

(2) Under a load of internal pressure, the pressure between the grain and the case has an important influence on the hoop strain on the inner surface of the grain. The greater the pressure is, the smaller the hoop strain is. Either increasing the circumferential modulus of the case cylinder or decreasing the m number of the grain can effectively reduce the hoop strain on the inner surface of the grain. Especially decreasing m number, its effect is more obvious, but it also leads to diminishing the propellant mass amount of the motor

(3) For tactical motors in service at low temperature, medium-strength and high-modulus carbon fibers are prior materials to fabricate composite cases to increase the circumferential modulus of the case cylinder. During the working process of the motor, the hoop strain of the case can be measured, and the hoop strain on the inner surface of the grain can be monitored in real time also. The curve of the strain changes over time can be obtained, which can provide a basis of the detection index for the safety assessment of the motor

Data Availability

As most of the data in this manuscript were related to trade secrets, I cannot provide them completely. In the future, if necessary, I can share some data with reviewers or readers.

Conflicts of Interest

The authors declare that there is no conflict of interest regarding the publication of this paper.

Acknowledgments

This article was funded by the Xi'an Jiaotong University and the Natural Science Basic Research Program of Shaanxi Province 2021JQ-527.

References

[1] G. S. Tussiwand, V. E. Saouma, R. Terzenbach, and L. T. De Luca, "Fracture mechanics of composite solid rocket propellant grains: material testing," *Journal of Propulsion & Power*, vol. 25, no. 1, pp. 60–73, 2009.

[2] R. Marimuthu and B. Nageswara Rao, "Development of efficient finite elements for structural integrity analysis of solid rocket motor propellant grains," *International Journal of Pressure Vessels & Piping*, vol. 111, pp. 131–145, 2013.

[3] C. Wang, P. Cao, M. Tang, and W. Tian, "Study on properties prediction and braiding optimization of axial braided carbon/carbon composite," *Materials*, vol. 13, no. 11, p. 2588, 2020.

[4] I. D. Parsons, P. Alavilli, and A. Namazifard, "Coupled simulations of solid rocket motors," in *36th AIAA/ASME/SAE/ASEE Joint Propulsion Conference and Exhibit*, 2000.

[5] H. R. Cui, G. J. Tang, and Z. B. Shen, "Study on the viscoelastic poisson's ratio of solid propellants using digital image correlation method," *Propellants, Explosives, Pyrotechnics*, vol. 41, no. 5, pp. 835–843, 2016.

[6] K. F. Grythe and F. K. Hansen, "Diffusion rates and the role of diffusion in solid propellant rocket motor adhesion," *Journal of Applied Polymer Science*, vol. 103, no. 3, pp. 1529–1538, 2007.

[7] A. M. F. de Morais, J. A. R. Pinto, and J. A. S. Holanda, "Optimization of bondline properties of solid rocket motors," in

37th International Annual Conference of ICT, Karlsruhe, Germany, June, 2006.

[8] A. V. Cunliffe, "Fraction measurements-a tool to study cross-linking and ageing in composite propellants and PBXs," in *37th International Annual Conference of ICT*, Karlsruhe, Germany, June, 2006.

[9] C. Wang, M. Tang, W. Liu, and T. Zhu, "Study on microstructure characteristics of axially braided carbon/carbon composites based on SEM and Micro-CT," *Material*, vol. 13, no. 6, p. 1414, 2020.

[10] J. L. Zhao, *Mechanics Damage and Meso Numerical Simulation of Evolvement Processing Research for Composite Solid Propellant*, Second Artillery Engineering University, 2010.

[11] L. Zhongbing, F. Li, and Y. Li, "Calculation analysis for structural integrity of solid propellant grains under high overload," *Journal of Solid Rocket Technology*, vol. 26, no. 2, pp. 12–16, 2003.

[12] Z. Liu, Y. Zhou, and B. Zhang, "Structural integrity analysis on grains of solid rocket motor at low temperature ignition," *Journal of Solid Rocket Technology*, vol. 38, no. 3, pp. 351–354, 2015.

[13] H. T. Chu and J. H. Chou, "Effect of cooling load on the safety factor of propellant grains," *Journal of Propulsion & Power*, vol. 29, no. 1, pp. 27–33, 2013.

[14] B. Wasistho, "3D coupled simulations of flexible inhibitors in the RSRM," in *41st AIAA/ASME/SAE/ASEE Joint Propulsion Conference & Exhibit*, 2005.

[15] R.-x. Chen, "Effect of case stiffness on the grain strength when applied internal pressure," *Journal of Solid Rocket Technology*, vol. 34, no. 1, pp. 101–104, 2011.

[16] R.-x. Chen and Y. Chen, "Relationship between grain inner surface train and case strain," *Journal of Solid Rocket Technology*, vol. 36, no. 6, pp. 763–765, 2013.

[17] R.-x. Chen, "Deformation analysis on solid motor composite case," *Journal of Solid Rocket Technology*, vol. 29, no. 4, pp. 266–268, 2006.

[18] P. Bose and K. M. Pandey, *Analysis of Anisotropy and Viscoelastic Properties of Composite Solid Propellant and Its Suitability for Use in Solid Rocket under Field Deployment*, International Review of Aerospace Engineering, 2012.

[19] K. Deng, L. Zhang, A. Pang, R. Yu, and P. Xin, "Analysis on structural integrity of a free loading solid propellant grains under ignition loading at low temperature," *Journal of Solid Rocket Technology*, vol. 41, no. 4, pp. 428–434, 2018.

[20] B. Zeller, "Solid propellant grain design," *Solid Rocket Propulsion Technology*, pp. 35–84, 1993.

[21] A. Kumar, A. Chakrabarti, and P. Bhargava, "Finite element analysis of laminated composite and sandwich shells using higher order zigzag theory," *Composite Structures*, vol. 106, pp. 270–281, 2013.

[22] A. Kumar, A. Chakrabarti, and P. Bhargava, "Vibration of laminated composites and sandwich shells based on higher order zigzag theory," *Engineering Structures*, vol. 56, pp. 880–888, 2013.

[23] A. Kumar, A. Chakrabarti, P. Bhargava, and R. Chowdhury, "Probabilistic failure analysis of laminated sandwich shells based on higher order zigzag theory," *Journal of Sandwich Structures & Materials*, vol. 17, no. 5, p. 1099636215577368, 2015.